Neuron, Vol. 20, 1219–1229, June, 1998, Copyright ©1998 by Cell Press

Synaptic Defects and Compensatory Regulation of Inositol Metabolism in Inositol Polyphosphate 1-Phosphatase Mutants

Jairaj K. Acharya,* Pedro Labarca,*† Ricardo Delgado,*† Kees Jalink,* and Charles S. Zuker*‡
*Howard Hughes Medical Institute
and Departments of Biology and Neurosciences
University of California, San Diego
La Jolla, California, 92093
†Centro De Estudios Cientificos De Santiago
Departamento de Biologia
Facultad de Ciencias
Universidad de Chile
Santiago
Chile

Summary

Phosphoinositides function as important second messengers in a wide range of cellular processes. Inositol polyphosphate 1-phosphatase (IPP) is an enzyme essential for the hydrolysis of the 1-phosphate from either Ins(1,4)P_2 or Ins(1,3,4)P_3. This enzyme is Li^+ sensitive, and is one of the proposed targets of Li^+ therapy in manic-depressive illness. *Drosophila ipp* mutants accumulate IP_2 in their system and are incapable of metabolizing exogenous Ins(1,4)P_2. Notably, *ipp* mutants demonstrate compensatory upregulation of an alternative branch in the inositol-phosphate metabolism tree, thus providing a means of ensuring continued availability of inositol. We demonstrate that *ipp* mutants have a defect in synaptic transmission resulting from a dramatic increase in the probability of vesicle release at larval neuromuscular junctions. We also show that Li^+ phenocopies this effect in wild-type synapses. Together, these results support a role for phosphoinositides in synaptic vesicle function in vivo and mechanistically question the "lithium hypothesis."

Introduction

Receptor-mediated activation of phospholipase C (PLC) results in the generation of the two second messengers inositol 1,4,5-trisphosphate (Ins[1,4,5]P_3) and diacylglycerol (DAG). Ins(1,4,5)P_3 plays its primary role by mobilizing Ca^{2+} from intracellular stores (Streb et al., 1983; Berridge and Irvine, 1989), and DAG mediates its action by activating protein kinase C (PKC) (Nishizuka, 1992; Ranganathan et al., 1995). Together, these two signaling molecules control a wide range of cellular processes (Berridge, 1993). The termination of the signaling activity of Ins(1,4,5)P_3 is mediated by specific dephosphorylation/phosphorylation reactions (Figure 1). For example, InsP_3 is dephosphorylated by inositol polyphosphate 5-phosphatase to form Ins(1,4)P_2. Alternatively, Ins(1,4,5)P_3 can be phosphorylated by an Ins(1,4,5)P_3 3-kinase to form Ins(1,3,4,5)P_4. Ins(1,3,4,5)P_4 has been shown to gate Ca^{2+} entry at the plasma membrane (Shears, 1992) and is also a precursor for the biosynthesis of InsP_5 and InsP_6. InsP_5 and InsP_6 comprise the bulk of the mammalian inositol polyphosphates and have recently been implicated in the regulation of ion channels (Shears, 1996).

Inositol polyphosphate 1-phosphatase (IPP) is a magnesium-dependent and lithium-sensitive enzyme that catalyzes the removal of 1-phosphate from Ins(1,4)P_2 and Ins(1,3,4)P_3 (Inhorn and Majerus, 1988; Gee et al., 1988; York et al., 1994). A number of mammalian IPPs have been cloned and show a great deal of sequence conservation and functional similarity. It has been proposed that sequential dephosphorylation of Ins(1,4,5)P_3 by 5-phosphatases, IPP, and inositol monophosphatase is the major route of recycling of inositol from Ins(1,4,5)P_3 in animal cells (Shears, 1992; Figure 1, bold arrows). Inositol regeneration from Ins(1,3,4,5)P_4 occurs by the successive action of 5-phosphatase, IPP, inositol 3- and 4-phosphatases, and inositol monophosphatase. The breakdown of Ins(1,3,4)P_3 is mediated primarily by IPP, except in the bovine brain, where hydrolysis by a 4-phosphatase has been demonstrated to be the predominant route (Figure 1, broken lines; Bansal et al., 1987).

Given the central role of inositol phosphates in signaling, it may be expected that their levels and metabolism are tightly controlled in the cell. Although much is known about the biochemistry of these pathways in vitro, little is known about the in vivo mechanisms that orchestrate and regulate phosphoinositide availability and turnover. Indeed, a number of recent studies have demonstrated that phosphoinositide availability plays an important and direct role in the functioning and regulation of PIP_2-mediated signaling cascades, and that failure to properly regulate components of these pathways can have devastating consequences on cellular function. For instance, hyperactivation of PKC may lead to uncontrolled cell growth and tumorigenesis, while uncontrolled signaling from a PLC-mediated pathway can lead to calcium cytotoxicity and metabolic dysfunction (Chow et al., 1988; Geffner et al., 1988; Parissenti et al., 1996; Timar et al., 1996). The therapeutic effects of lithium in the management of manic-depressive illness are thought to result from the inhibition of two of the phosphatases involved in the pathway: inositol monophosphatase and IPP (Berridge et al., 1989; Majerus, 1992). Inhibition of these enzymes has been proposed to lead to a depletion of inositol pools and a corresponding decline in the levels of PIP_2. The "lithium hypothesis" states that the decrease in the levels of PIP_2 would be accompanied by a substantial decrease in PLC-based PIP_2 signaling and a concomitant reduction in neuronal excitation. Such reduction in signaling would then be responsible for the therapeutic effect of lithium in controlling the manic state of bipolar disorder.

Genetic analysis of inositol phosphate metabolic pathways has been very limited. In mammals, perhaps the only example is Lowe's Oculocerebrorenal Syndrome (LOS), a human genetic disorder linked to a mutation in a type II form of inositol polyphosphate-5-phosphatase

‡To whom correspondence should be addressed.

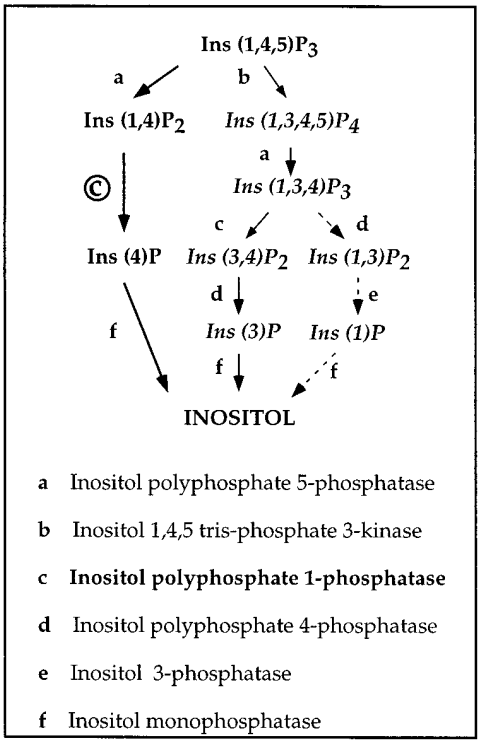

Figure 1. Metabolism of Ins(1,4,5)P_3

The arrows in bold indicate the predominant pathway of Ins(1,4,5)P_3 metabolism in most animal tissues (Majerus, 1992; Shears, 1992). Ins(1,3,4)P_3 is hydrolyzed to Ins(3,4)P_2 by IPP in all animal tissues studied except *Drosophila* (this study). The broken arrows indicate the likely route of Ins(1,3,4)P_3 breakdown in the *ipp* mutants. The enzymes catalyzing the reactions have been indicated, and the reaction catalyzed by *Drosophila* IPP is highlighted.

(Attree et al., 1992; Zhang et al., 1995; Majerus, 1996; Lin et al., 1997; Nussbaum et al., 1997). LOS is characterized by growth and mental retardation, cataracts, glaucoma, and renal tubular acidosis. How this mutation leads to the wide range of phenotypes seen in affected patients, or how it influences inositol metabolism in vivo, is unclear. In efforts to study the function and regulation of PIP_2 metabolism in vivo, we have been carrying out a genetic dissection of this process in *Drosophila*, a system well suited for comprehensive genetic studies. We have been using phototransduction, a phosphoinositide-mediated, Ca^{2+}-regulated signaling pathway, as the platform for these studies. We report here the isolation and characterization of *Drosophila ipp* mutants. We demonstrate that mutant flies have defective inositol metabolism, have compensatory changes that allow them to metabolize Ins(1,3,4)P_3, and manifest a neurologic *Shaker*-like phenotype. We used electrophysiology to map the basis of this neurological phenotype and demonstrate a defect in synaptic transmission due to a defect in synaptic vesicle release.

Results

Isolation of the *Drosophila* IPP

Drosophila phototransduction is a phosphoinositide-mediated G protein–coupled signaling cascade that utilizes PLC as the effector molecule. Several eye-specific enzymes involved in phosphoinositide signal transduction, such as phospholipase C (*norpA*), CDP-DAG synthase (*eye-CDS*), DAG-kinase (*rdgA*), and PI-transfer protein (*rdgB*), have been isolated from *Drosophila* (Ranganathan et al., 1995). In a screen designed to identify genes abundantly expressed in the fly retina, we isolated a *Drosophila* homolog of mammalian inositol polyphosphate 1-phosphatase. Figure 2 shows a diagram of the genomic structure and deduced amino acid sequence of the *Drosophila ipp* gene. *Drosophila* IPP displays 40% amino acid identity and 53% similarity with the mammalian IPPs, including human (York et al., 1993), bovine (York and Majerus, 1990), and mouse (Okabe and Nussbaum, 1995). The *Drosophila* protein shows significant sequence divergence in the area comprising the substrate recognition site (residues 281–320), with 18 amino acid substitutions over this small region (Figure 2A). In contrast, the mammalian forms differ by only two residues over the same interval (see next section).

To examine the tissue and developmental profile of expression of the *Drosophila* IPP protein, we generated polyclonal antibodies against overproduced protein and used them in tissue sections and Western blots. The protein is ubiquitously expressed throughout development and is present in all tissues examined, with maximal levels seen in the adult head and retina (Figure 3A). We also assayed IPP activity in extracts from different tissues and developmental stages and found a corresponding distribution, with maximal activity in the adult retina and head (Figure 3B). This profile of expression is consistent with a general role for IPP in inositol metabolism.

Drosophila IPP Displays Novel Substrate Specificity

Because the *Drosophila* IPP is the least conserved member of the IPP family (Figure 2), we set out to investigate whether these difference in primary sequence translate into fundamental differences in the properties of the enzyme. IPP is a Mg^{2+}-dependent and Li^{+}-sensitive enzyme that catalyzes the removal of 1-phosphate from Ins(1,4)P_2 and Ins(1,3,4)P_3 (Inhorn and Majerus, 1988; Gee et al., 1988; York et al., 1994). We overexpressed the *Drosophila* protein in *E. coli*, and the soluble active enzyme was purified to homogeneity using ion exchange and gel filtration chromatography (see Experimental Procedures) (Figure 3C). Purified IPP hydrolyzed inositol 1,4-bisphosphate to inositol-4-phosphate with a K_m of 2.5 μM and a V_{max} of 36 μmol/min/mg protein. This compares favorably to the activity of the mammalian enzyme. We next analyzed the sensitivity of Ins(1,4)P_2 hydrolysis to lithium. The activity of the pure enzyme was completely inhibited by 2 mM LiCl (Figure 3D), in line with the observed sequence conservation at the metal-binding site (Figure 2A). Surprisingly, the *Drosophila* enzyme could not hydrolyze Ins(1,3,4)P_3, even when we increased the concentration of enzyme by 50-fold (to 1 μg/ml) in the assay and used 100 μM substrate. In contrast, the mammalian IPPs efficiently dephosphorylate this substrate (Figure 1).

Because the recombinant *Drosophila* enzyme did not hydrolyze the 1-phosphate from Ins(1,3,4)P_3, we next assayed *Drosophila* extracts for their ability to hydrolyze this substrate. Table 1 shows that, much like the recombinant IPP, fly extracts cannot appreciably metabolize

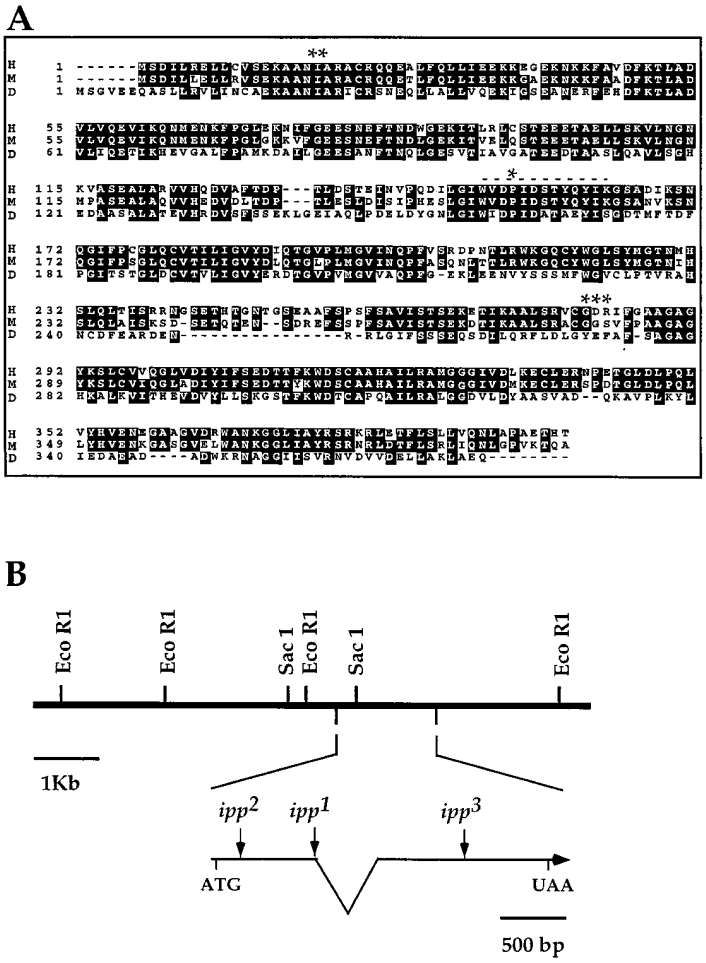

Figure 2. Structure of *Drosophila* IPP

(A) Shown is a collinear alignment of the deduced amino acid sequence of IPP from human (H), mouse (M), and *Drosophila* (D). Amino acids are designated by the single letter code. *Drosophila* IPP is the least conserved member of this family. The asterisks at residues 71, 163, and 273 indicate the location of the nucleotide changes in the three mutant alleles (*, *ipp*^{1} ;**, *ipp*^{2}; and ***, *ipp*^{3}). Dashed lines indicate the metal binding site. (B) *ipp* gene structure. The *Drosophila* gene has a single intron of 284 nucleotides. The *ipp*^{1} allele eliminates the splice donor site and creates a complete null mutation.

Ins(1,3,4)P_3, yet they efficiently metabolize Ins(1,4,5)P_3 and Ins(1,4)P_2. As expected, bovine extracts can dephosphorylate both Ins(1,4,5)P_3 and Ins(1,3,4)P_3. These results predict that the primary route of InsP_3 metabolism in *Drosophila* is via Ins(1,4)P_2 (Figure 1, bold arrows) and suggest that defects in IPP function may have a substantial impact on inositol phosphate metabolism in vivo.

Isolation of *ipp* Mutants

The *Drosophila ipp* gene maps to the third chromosome at position 88A1–2. We carried out a chromosomal walk over this area, fine mapped the locus to a 40 kb interval, and set out to isolate mutants defective in this gene. A difficulty in setting up a screen for mutations in *ipp* is the lack of a clear, predictable phenotype that defines its loss of function. Because of this concern, we used a screening strategy that was based on the loss of IPP antigen on immunoblots (Dolph et al., 1993). The advantage of this screen is that it does not rely on a hypothetical physiological or behavioral defect but only on the presence or absence of IPP protein. Single heads from flies heterozygous for a large chromosomal deficiency that deletes the *ipp* gene and a mutagenized third chromosome were screened for the loss of IPP by Western blots. Analysis of 4368 lines yielded three alleles: *ipp*^{1}, *ipp*^{2}, and *ipp*^{3} (Figures 2 and 4B).

Using the polymerase chain reaction (PCR), we isolated the *ipp* gene from each of the mutant lines and determined their entire nucleotide sequence. *ipp*^{1} contains a G→A change in the donor splice site at nucleotide 578; this results in a null mutation. *ipp*^{2} contains a T→A change at nucleotide 71, resulting in the substitution of a conserved isoleucine to a lysine at residue 24; this mutant expresses ~2% of the normal levels of protein. *ipp*^{3} contains an 11 nucleotide insertion at position 902, resulting in a frameshift at amino acid residue 273.

ipp Mutants Accumulate InsP_2

When we assayed mutant extracts for their ability to hydrolyze Ins(1,4)P_2, no hydrolysis was detected in any of the three alleles (Figure 4C). Furthermore, when mutant extracts were incubated with labeled Ins(1,4,5)P_3, >95% of the label was recovered as inositol bisphosphate, whereas in extracts from control flies, >95% of the label was recovered as inositol. This defect is due exclusively to the loss of IPP, since introduction of a wild-type copy of the *ipp* gene into the mutant hosts restored normal function.

Since IPP appears essential to metabolize Ins(1,4)P_2, we reasoned that *ipp* mutants may display a significant accumulation of InsP_2. Wild-type and mutant flies were fed tritiated inositol for 6 hr and analyzed for inositol

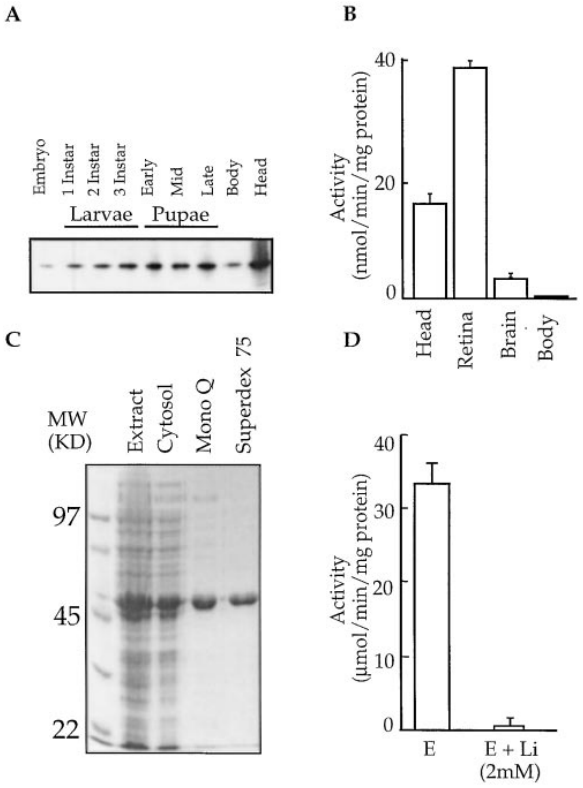

Figure 3. *Drosophila* IPP Is Ubiquitously Expressed

(A) IPP is expressed throughout development. Shown is a Western blot containing 20 μg of soluble protein extracts from different tissues and stages of development.

(B) Ins(1,4)P_2 phosphatase activity is highly enriched in the nervous system. Assays were initiated by the addition of cytosolic extracts to a buffer mixture containing tritiated Ins(1,4)P_2 exactly as described in the Experimental Procedures.

(C–D) IPP activity is inhibited by Li^+.

(C) *Drosophila* IPP was expressed in *E.coli* using the pET3a expression system (Studier and Moffat, 1986) and purified to apparent homogeneity on FPLC using Mono Q ion-exchange and Superdex 75 gel-filtration columns.

(D) Purified IPP is completely inhibited by 2 mM LiCl (n = 6).

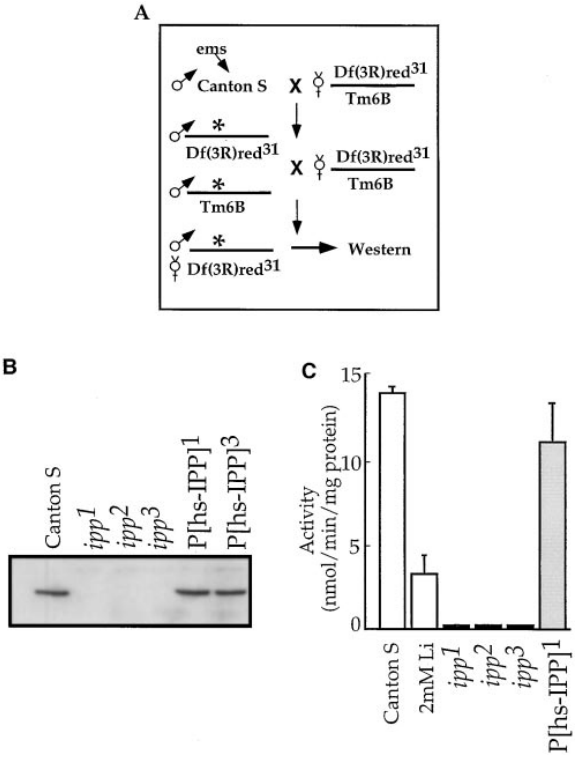

Figure 4. *ipp* Mutants Are Incapable of Metabolizing Ins(1,4)P_2

(A) Genetic scheme used to generate *ipp* mutants. The three mutant alleles were identified by a Western blot screen of 4368 mutagenized lines (Dolph et al., 1993).

(B and C) IPP expression and activity is abolished in *ipp* mutants. Western blots of protein extracts from wild-type and mutant lines. Also shown are two transgenic lines carrying the IPP gene under the control of the heat shock promoter, either in the ipp^1 (P[hs-IPP]^1) or ipp^3 (P[hs-IPP]^3) background. This construct fully rescues the (B) IPP protein and (C) enzymatic activity defects. In (B), each lane contains protein extracts from a single fly head. Activity assays were performed with 5 μg of head extracts in 50 μl of reaction volume as described in the Experimental Procedures. ipp^1, ipp^2, and ipp^3 have no $InsP_2$ hydrolyzing activity, and introduction of a wild-type IPP under control of a heat-shock promoter, P[hs-IPP], rescues this defect. The activity in the wild-type extract is inhibited >80% by 2 mM lithium.

phosphates. As predicted, *ipp* mutants have a vast increase of $InsP_2$ in their system; measured ratios of $InsP_2$/$InsP_1$ revealed a 300% increase in the levels of Ins(1,4)P_2 in the ipp^1 mutants (Figure 5A). Together, these results substantiate a biochemical deficit in the mutant lines, and demonstrate that *ipp* encodes the major IPP in *Drosophila*.

ipp Mutants Compensate for the Loss of the Major Metabolic Route

Because *ipp* mutants cannot hydrolyze Ins(1,4)P_2, and because the Ins(1,3,4)P_3 route is very inefficient in wild-type *Drosophila*, we questioned how the *ipp* animals manage Ins(1,4,5)P_3 signaling. We performed two types of studies. First, we examined signaling in a prototypical PLC-based signaling cascade. Second, we examined the *ipp* mutants for $InsP_3$ turnover.

As an example of a well-characterized PLC signaling pathway, we studied phototransduction in *Drosophila*. In this cascade, light activation of rhodopsin activates a heterotrimeric G protein of the Gq family, which activates a PLC encoded by the *norpA* gene. Detailed electrophysiological analysis of wild-type and mutant flies demonstrated that *ipp* mutants are indistinguishable

Table 1. *Drosophila* and Bovine Brain Differ in InsP Metabolism

	Ins(1,4,5)P_3	Ins(1,4)P_2	Ins(1,3,4)P_3
Drosophila head extract	>80%	>80%	<1%
Bovine brain cytosol	>80%	ND	>80%

Protein extracts isolated from *Drosophila* heads (5 μg) or bovine brain cytosol (8 μg) were incubated with tritiated substrates (20 μM) in a 50 μl reaction for 30 min at 37°C. The incubation was stopped by adding 1 ml of ice-cold water, and the reaction products were separated on a Dowex-formate AG-1X8 column as described in the Experimental Procedures. Numbers shown reflect percent of substrate hydrolyzed by each extract in at least five independent experiments. ND, not determined.

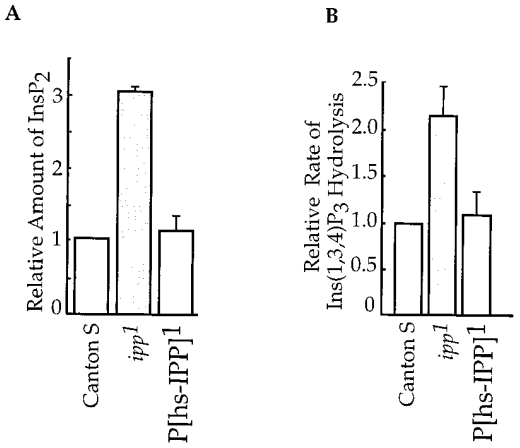

Figure 5. *ipp* Mutants Have Altered Inositol Metabolism

(A) *ipp*^{1} mutants accumulate $InsP_2$ in their system. Canton S, *ipp*^{1}, and P[hs-IPP]^1 flies were fed [^{3}H] inositol for 6 hr. The flies were quickly frozen in liquid nitrogen and homogenized in 0.4 N perchloric acid. The inositol and inositol phosphates were separated on Dowex-formate columns as described (Berridge et al., 1983; Shayman et al., 1987). The graph shows the relative amounts of $InsP_2$ in each genetic background (n = 3). *ipp* mutants have a 3-fold increase in the steady-state levels of $InsP_2$. However, this is fully reversed in *ipp* mutants carrying a wild-type transgene.

(B) *ipp*^{1} flies have compensatory upregulation of inositol metabolism. Head extracts (50 μg) from Canton S, *ipp*^{1}, and P[hs-IPP]^1 flies were incubated with [^{3}H] Ins(1,3,4)P_3 (60 μM) at 37°C for 5–15 min in 20 μl of buffer as described in the Experimental Procedures. The reaction was terminated by adding 1 ml of ice-cold 0.4 M ammonium formate containing 0.1 M formic acid. The [^{3}H] Ins(1,3,4)P_3 breakdown products were fractionated on Dowex-formate columns. The specific activity of each genotype was normalized to the wild-type activity (n = 6).

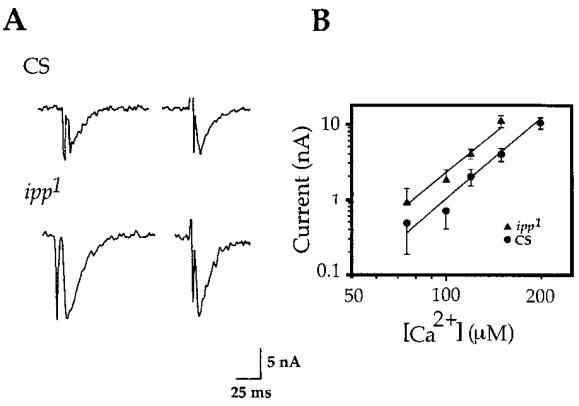

Figure 6. *ipp* Mutants Have Defects in Evoked Responses at the Larval NMJ

(A) Shown are typical records of postsynaptic responses from larval NMJ in CS and *ipp*^{1} mutants in the presence of 150 μM extracellular Ca^{2+}. The stimulation and recording paradigm was exactly as described in the Experimental Procedures (Jan and Jan, 1976; Delgado et al., 1992, 1994). Average amplitudes: CS = 4.2 ± 1.2 nA, *ipp*^{1} = 11.3 ± 3.5 nA.

(B) Double log plot of response amplitudes versus calcium concentration. Excitatory postsynaptic currents were recorded in the presence of 75, 100, 120, 150, and 200 mM extracellular Ca^{2+} (CS, circles; *ipp*^{1}, triangles); these concentrations were chosen since they represent the range at which synaptic function and plasticity is normally assayed in larval NMJ. While there is a shift to the left in the *ipp* responses, the slopes of both curves are indistinguishable from each other, demonstrating similar Ca^{2+} dependence of transmitter release (see text for details).

from wild-type controls (data not shown). We also generated double mutants between *ipp* and several genes encoding components of inositol phosphate metabolism in photoreceptor cells. These included DAG-kinase (*rdgA*; *ipp*), CDP-DAG synthase (*eye-CDS*; *ipp*), and PI-transfer protein (*rdgB*; *ipp*). In no case did we detect an enhancement or suppression of the single mutant phenotypes by the inclusion of the *ipp* allele (data not shown; see Discussion). We reasoned that if $InsP_3$ metabolism is of fundamental importance for such a wide range of cellular functions, then perhaps compensatory mechanisms exist in the *ipp* mutants. Since *ipp* mutants failed to metabolize Ins(1,4)P_2 in vivo and in vitro, we examined whether the phosphorylation route of $InsP_3$ metabolism, a branch not appreciably utilized in wild-type flies (Figure 1), was altered in the mutants. Indeed, we found a significant increase in the rate of hydrolysis of Ins(1,3,4)P_3 in the mutants (Figure 5A). This upregulation is fully dependent on the loss of IPP activity, because mutant animals carrying a rescue construct resemble wild-type controls. Taken together, these results demonstrate metabolic compensation in vivo and highlight the exceptional capacity of the organism to partially accommodate the loss of function of a key enzyme in this pathway.

ipp Mutants Are Hyperexcitable

The results presented above suggested that cells display incredible tolerance to changes in inositol phosphate metabolites, including significant increases in the levels of $InsP_2$. A strong indication that *ipp* mutants had a physiological defect came from examination of their behavior. The flies showed mild but reproducible hyperexcitability: they displayed the characteristic twitching of the legs seen in *Shaker*-like mutants while recovering from the anesthetic effects of diethyl ether (relative ranking: $Hk \approx Sh^{102} >> ipp^1 > eag^1$). Since phosphoinositides have been implicated in a wide range of neuronal functions, including synaptic vesicle function (De Camilli et al., 1996), we analyzed synaptic transmission in control and mutant animals by performing electrophysiological recordings at the larval neuromuscular junction (NMJ). We recorded from the third instar larval ventral longitudinal muscle 6 (from segments A2 or A3) using a two-electrode voltage-clamp configuration. We chose this preparation because its behavior has been well described (Jan and Jan, 1976; Crossley, 1978; Campos-Ortega and Hartenstein, 1985; Zhong and Wu, 1990; Budnik et al., 1990; Delgado et al., 1992; Delgado et al., 1994) and can be used to reliably analyze both evoked and spontaneous transmitter release, as well as many aspects of synaptic plasticity (Baumgartner et al., 1996; Broadie et al., 1997; Petersen et al., 1997).

Examination of postsynaptic end-plate currents triggered by stimulation of the nerves demonstrated that *ipp* mutants have evoked responses that are severalfold larger than those of wild-type controls (Figure 6A). This increase is maintained at a range of concentrations of extracellular calcium (Figure 6B) and is not due to changes in the calcium dependence of transmitter release. This is best illustrated by analyzing the slope of

the log [Ca^{2+}] versus log [amplitude] plot; the slope of this function is thought to represent the number of calcium ions required to trigger vesicle fusion and is ~3.5 in both genotypes (CS: 3.6 ± 0.2; *ipp*: 3.5 ± 0.3, n = 4). This is in good agreement with previous estimates (Petersen et al., 1997). We also examined the ultrastructure of the NMJ in both genotypes using electron microscopy and immunofluorescence stainings (Poodry and Edgar, 1979; Jia et al., 1993; Thomas et al., 1997). There were no significant differences in the size or number of synaptic boutons or active zones between control and *ipp* mutant flies (data not shown).

At a mechanistic level, the large increase in the amplitude of evoked responses in *ipp* could be due to an increase in the number of docked vesicles, an increase in transmitter content per vesicle, an increase in the probability of release, or a combination of these defects. We therefore examined the size of the readily releasable pool using hypertonic shock, the size of each quantum by analyzing single release events, and the probability of release by determining the frequency of failures.

To functionally measure the size of the readily releasable pool in wild-type and mutant synapses, we used osmotic shock, a release protocol that does not depend on electrical activity or changes in intracellular calcium, to trigger quantal release from docked vesicles (Stevens and Tsujimoto, 1995; Rosenmund and Stevens, 1996). We applied a solution of 0.5 M sucrose in the vicinity of synaptic boutons and recorded the ensuing end-plate currents (Broadie et al., 1995). We also examined the relative rate of vesicle recycling by measuring the time required to recover the pool of readily releasable vesicles using a paired application paradigm (Stevens and Tsujimoto, 1995). Our results (Figure 7 and data not shown) indicate that wild-type and mutant synapses have similarly sized pools of readily releasable vesicles and similar rates of recycling.

We next determined the size of an individual quantum in wild-type and mutant larvae by recording minis under conditions in which only one or zero events are produced. In essence, we used low temperature incubations and examined events where the frequency of failures in wild-type and mutant synapses was >90%. The results confirmed that wild-type and *ipp* mutants have similar miniature postsynaptic end-plate current amplitudes. We also examined the frequency and size of spontaneous end-plate currents at 25°C and detected no significant differences between control and mutant animals (CS: current integral = 18.7 ± 1.7 pC, frequency = 5.1 ± 1.0 minis/s; *ipp*^{1}: current integral = 15.9 ± 1.1 pC, frequency = 3.1 ± 0.5 minis/s). We hypothesized that the *ipp* synaptic phenotype may be due to an increase in the probability of release. We studied the probability of release in wild-type and mutant synapses by examining the frequency of synaptic failures following low frequency nerve stimulation under conditions of low extracellular calcium. Figure 8 demonstrates that the fraction of failures in *ipp* flies is dramatically reduced compared to wild-type controls. Wild-type synapses failed to trigger release in ~75% of the trials (n = 4 larvae, at least 100 trials each), whereas failures in *ipp* mutants occurred in only ~30% of the trials. Since the release of quanta is well fitted by a Poisson distribution in this preparation (Petersen et al., 1997), we applied the method of failures

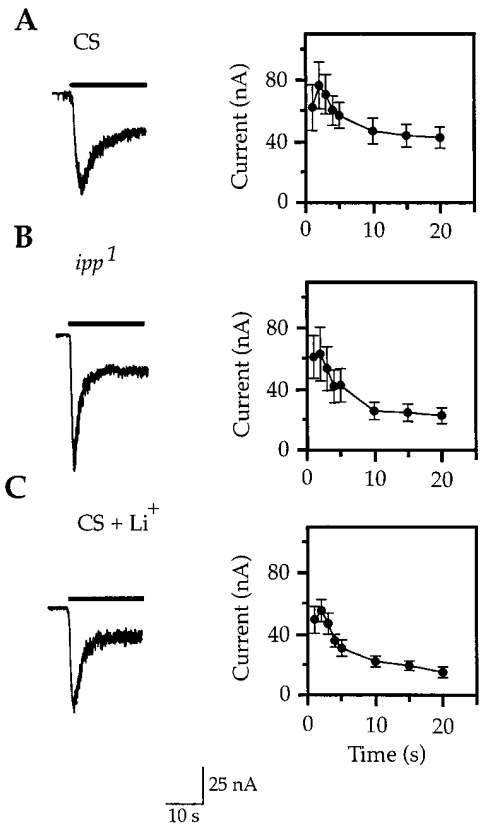

Figure 7. Osmotic Release of Neurotransmitter

Osmotic release of neurotransmitter was induced by application of a hyperosmotic solution containing 500 mM sucrose (Stevens and Tsujimoto, 1995; Rosenmund and Stevens, 1996). Extra caution was taken to insure that we recorded from the same segment, under the same conditions, in all larvae; we performed local superfusion of a limited area as described in the Experimental Procedures. The left panels show representative examples of current responses during a 20 s pulse of hyperosmotic solution in (A) CS, (B) *ipp*^{1}, and (C) CS larvae in the presence of 10 mM LiCl. The black bar on top of each record indicates the period of exposure to the hyperosmotic solution. The right panels show the average time course of responses for each genotype (CS, n = 13, *ipp*^{1} n = 10, CS + Li^+, n = 4). There were no significant differences between any of the genotypes. For studies of recycling/recovery, we ensured that responses had returned to baseline before application of the second shock ($\tau \approx 10$ s).

to calculate quantal content. Quantal content (m) in Canton S controls is 0.29 ± 0.04, and the probability of release is 0.25 (P_1 = 0.22 and P_2 = 0.031). In contrast, quantal content in *ipp* is 1.17 ± 0.1, and the probability of release is 0.69 (P_1 = 0.36, P_2 = 0.22, P_3 = 0.086). We also used the frequency histograms shown in Figure 8 to calculate quantal content from the experimental data; both methods produced very similar estimates (CS: m = 0.34 ± 0.05 and P_1 = 0.24, P_2 = 0.04; *ipp*^{1}: m = 1.35 ± 0.2 and P_1 = 0.35, P_2 = 0.26). Taken together, these data demonstrate that the increase in postsynaptic responses in *ipp* mutants is not the result of changes in the Ca^{2+} dependence of release, nor is it due to an increase in the size of the readily releasable pool or an increase in the size of individual quantum. Instead, the phenotype is due to a notable enhancement in the probability of vesicle release.

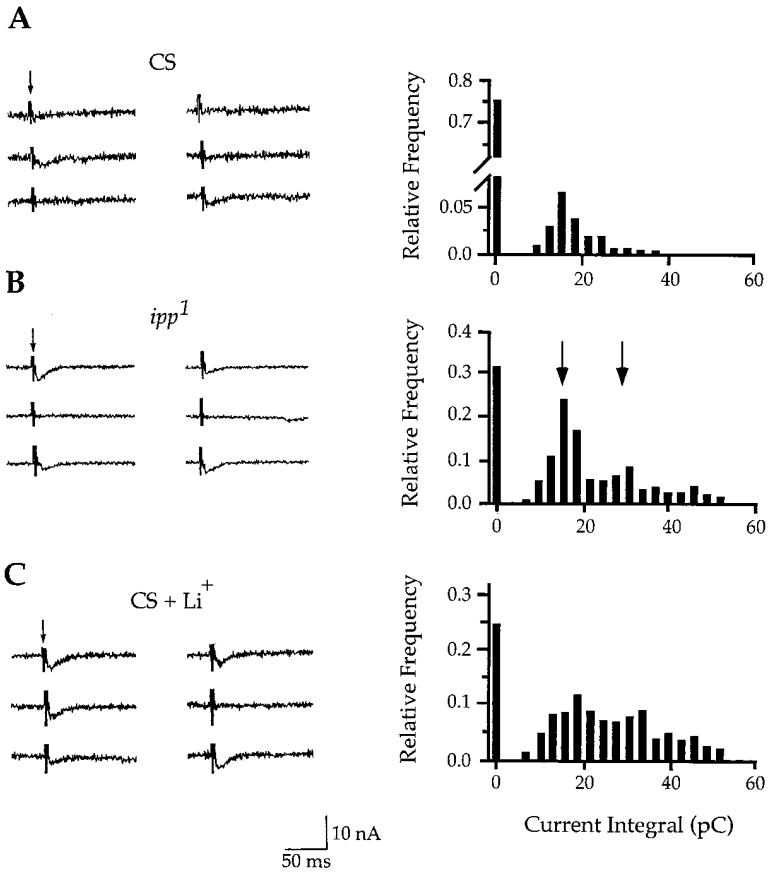

Figure 8. Synaptic Transmission is Defective in *ipp* Mutants

Postsynaptic currents were evoked by low frequency nerve stimulation (0.05 Hz) in 75 μM extracellular Ca^{2+}. In each experiment, the fraction of failures was estimated from at least 100 trials and at least four different larvae. Individual frequency histograms (not shown) were not statistically different than the summed averages. The left panels show sample current traces of evoked responses for each genotype: (A) CS, (B) *ipp*^{1}, and (C) CS + Li^+. The right panels show the corresponding current integral/frequency histograms.

(A) The major bar at 0 indicates the frequency of failures obtained directly from the experimental records (n = 417 trials). The peak at 17 pC likely corresponds to the unitary event. Using Poisson statistics, quantal content is 0.29 ± 0.04, and P_1, the probability of release of one quantum, is 0.22. This is in fair agreement with estimates from experimental data shown in the histogram, which predicts m = 0.34 and P_1 = 0.24. The probability of release of two quanta is 0.03. Note that the average integral of spontaneous currents at low temperature is similar to the average of the integral currents in CS at 75 μM Ca^{2+}, at which the probability of release of a quantum is very low. This coincidence supports the idea that the peak in the histogram in Figure 8A corresponds to a single event (quantum).

(B) The probability of release in *ipp*^{1} is significantly larger than in CS (0.69 versus 0.25) (n = 248). Arrows indicate the location of one and two events. The probability of release of one, two, or more quanta obtained from the experimental data is in good agreement with the predictions of the Poisson distribution (see text for details).

(C) CS motor end plates were incubated for 30 min in an external solution made of 118 mM NaCl, 10 mM LiCl, 2 mM KCl, 4 mM $MgCl_2$, 0.075 mM $CaCl_2$, 36 mM sucrose, and 5 mM HEPES (pH 7.0). The frequency of failures in this case was 0.25 ± 0.05, and the quantal content was m = 1.38. These values are notably different from CS control values but are not significantly different from *ipp*^{1} values. The histogram was built by data derived from 439 trials in five different larvae. The probabilities of release of 0, 1, 2, or more quanta obtained from the experimental data are in good agreement with those predicted by the Poisson distribution. The frequency of failures in *ipp*^{1} mutants incubated with Li^+ was not statistically different from that of *ipp* controls (0.39 ± 0.08 versus 0.31 ± 0.09).

ipp Mutants Have Defects in Synaptic Function

Since synaptic vesicle fusion and transmitter release critically depend on intracellular calcium, the increase in the probability of release seen in *ipp* mutants could be partly due to defects in calcium homeostasis resulting from defects in $InsP_3$ metabolism (i.e., higher basal levels of calcium). Alternatively, this phenotype could be a reflection of a fundamental defect in synaptic vesicle function and/or mobilization. To help address this issue, we studied responses under conditions where the probability of release, both in wild-type and in mutant animals, is high (tetanic stimulation at 200 μM extracellular Ca^{2+}, where no failures are observed). During a tetanus, normal synapses display a characteristic increase in the size of the postsynaptic response due to enhanced presynaptic release resulting from successive rises in the levels of intracellular calcium (Figure 9A). Remarkably, *ipp* mutants are totally incapable of maintaining a sustained response to a prolonged stimulus (10 Hz for 50 s; Figure 9B): they reach a plateau much faster than control synapses and decay during the stimulus. Indeed analysis of the *ipp* responses demonstrated a progressive decrease in quantal content as the tetanus proceeds (see expanded traces under the individual response graphs). This depletion phenotype persisted even when wild type and mutants were compared over a range of Ca^{2+} concentration (see Figure 6B), including millimolar Ca^{2+} concentrations (data not shown). The defect is common to all *ipp* alleles, but mutant larvae carrying a wild-type *ipp* transgene show normal responses (data not shown). In sum, these results substantiate a defect in synaptic transmission in *ipp* mutants (perhaps due to a defect in vesicle mobilization) and suggest that the depression in signaling following prolonged stimulation may define important physiological changes during acute and chronic pharmacological inhibition of IPP in the nervous system (see next section).

Lithium Interferes with IPP In Vivo and Phenocopies the Synaptic Defect of *ipp* Mutants

The favored hypothesis for the action of lithium in the nervous system (manic-depressive psychosis) proposes that inhibition of the inositol monophosphatases leads to a decline in the pool of inositol and a corresponding

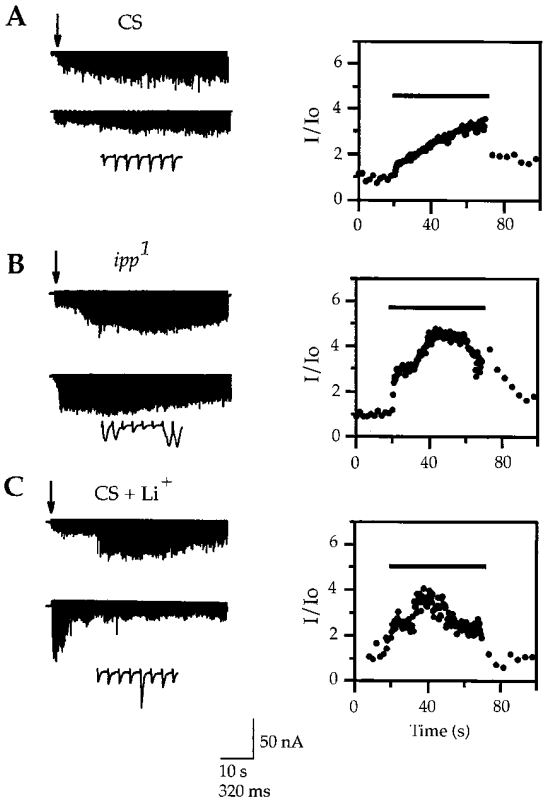

Figure 9. *ipp* Mutants Cannot Sustain Responses to Prolonged Tetanic Stimulation

Shown are typical traces of evoked responses (left) to a 10 Hz stimulus for 50 s in (A) CS (n = 6), (B) *ipp*^{1} (n = 9), and (C) CS + Li^+ larvae (n = 5). Each trace represents a single larva. The traces below the records show individual evoked postsynaptic currents at expanded time resolution. Note the reduced responses in *ipp*^{1} and CS + Li^+ animals. As expected, control animals display robust tetanic augmentation during the course of the experiment. However, *ipp* mutants, and animals exposed to 10 mM LiCl, cannot sustain responses. Similar responses to tetanic stimulation were recorded in CS in Li^+-free solution, after larval incubation in the Li^+-containing solution. The right panels show averaged, normalized responses (I/Io) from at least five motor end-plates, each from a different larva. SEMs have been omitted for clarity. At peak, SEM values were: CS = 3.5 ± 0.85 nA, *ipp*^{1} = 6.0 ± 1.4 nA, and CS + Li^+ = 4.0 ± 1.0.

decrease in the levels of PIP_2 and PIP_2-based signaling. Our findings that *ipp* mutants have severe synaptic defects suggested that pharmacological inhibition of IPP could phenocopy the *ipp* mutant phenotype and lead to significant defects in synaptic function and plasticity. Furthermore, since a number of components of the vesicle fusion/recycling machinery have recently been linked to inositol phosphates (De Camilli et al., 1996; McPherson et al., 1996; Fukuda and Mikoshiba, 1997), we wondered whether this pathway could be a biologically relevant target of lithium. We therefore tested the effect of acute lithium exposure on wild-type and *ipp* synapses. Remarkably, Li^+ phenocopies all aspects of the *ipp* mutant phenotype, including the increase in size of evoked responses, the decrease in synaptic failures, and the inability to sustain long tetanic stimulation (Figures 8C and 9C). In contrast, *ipp* mutants are resistant to equivalent treatment and exposure to Li^+ (e.g., fraction of failures: CS = 0.75, *ipp*^{1} = 0.31, *ipp*^{1} + Li^+ = 0.39; see Figure 8). Collectively, these data demonstrate that IPP is an important target of Li^+ in vivo and point to synaptic vesicle function as a critical candidate in the study of Li^+ action and its involvement in the management of psychiatric disorders.

Discussion

Inositol phosphates are important intracellular messengers in a wide range of signaling pathways. They also serve as reservoirs for phosphate and mineral storage. Cells utilize a variety of strategies to insure availability of inositol and related metabolites, including synthesis, uptake, and recycling. One of the most important inositol phosphates is Ins(1,4,5)P_3. It functions not only as a key messenger in mobilizing calcium from internal stores but also as a central intermediate in the synthesis of a wide range of additional signaling molecules.

The metabolism of Ins(1,4,5)P_3 operates via one of two pathways. On the one hand, it can be phosphorylated to generate Ins(1,3,4,5)P_4. On the other hand, it can be dephosphorylated to produce Ins(1,4)P_2. Inositol polyphosphate 1-phosphatase is a key enzyme in this latter branch. IPP is lithium sensitive and has been postulated to be one of the pharmacologically relevant targets of lithium therapy in the treatment of manic depression. In this study, we described the isolation of the *Drosophila ipp* gene and the characterization of *ipp* mutants.

We showed that Ins(1,3,4)P_3 is poorly metabolized in *Drosophila*, suggesting that the Ins(1,4)P_2 branch is the major route of Ins(1,4,5)P_3 metabolism. We also demonstrated that *ipp* mutant flies have no detectable inositol 1-phosphatase activity, are defective in inositol metabolism, and have a large increase in the steady-state levels of $InsP_2$ in their system. Unexpectedly, we found that phototransduction, a prototypical PLC pathway heavily dependent on phosphoinositide metabolism, is not affected in *ipp* mutants. This could be rationalized by assuming that inositol may not be limiting in these cells, arguably because of large pools due to the high demands for PIP_2 in photoreceptors (see Berridge and Irvine, 1989; Berridge, 1993).

Why are *ipp* mutant animals viable if they lack the primary route of $InsP_3$ metabolism? We showed that *ipp* mutants have a significant increase in the rate of breakdown of Ins(1,3,4)P_3, thus rerouting Ins(1,4,5)P_3 via the Ins(1,3,4,5)P_4 pathway. This compensatory change demonstrates exquisite biochemical plasticity in vivo and is likely to represent the alternate route for metabolizing the accumulated inositol polyphosphates in these flies.

We demonstrated that *ipp* mutants have defects in synaptic function due to an underlying defect in synaptic vesicle function. We used a number of electrophysiological strategies to pinpoint the nature of the defect and demonstrated that *ipp* mutants have a significant increase in the probability of synaptic vesicle release. These results are well aligned with recent studies linking inositol phosphates to the life cycle of secretory vesicles (see De Camilli et al., 1996; Fukuda and Mikoshiba,

1997). Because *ipp* mutants disrupt phosphoinositide metabolism, one would like to directly measure calcium levels in wild-type and mutant synapses. Unfortunately, this experiment is complicated by the very small size of presynaptic boutons in this preparation. We reasoned that if differences in intracellular calcium underlie the differences in probability of release, then wild-type synapses under conditions of very high probability of release may mimic *ipp*. This was not the case; *ipp* mutants were unable to maintain responses to a prolonged tetanus, whereas control animals displayed robust responses and a fully developed tetanic augmentation. In all, these findings suggested that inhibition of *ipp* may lead to changes in synaptic plasticity. Indeed, Li^+ application phenocopies the synaptic defects of *ipp* mutants. These results raise the possibility that the therapeutic effects of Li^+ in the management of manic depressive psychosis may be mediated by its action on synaptic vesicle function and prompt a reexamination of the "lithium hypothesis" and its significance in PLC signaling vis-a-vis synaptic transmission. Finally, the availability of this mutant highlights the need for a comprehensive dissection of inositol phosphate metabolism and function in vivo and makes it possible to design various genetic screens to identify additional components of these pathways.

Experimental Procedures

Cloning of *ipp*

A cDNA encoding the 3′ end (700 bp) of *ipp* was identified during screening of a retinal lambda Zap cDNA library for genes preferentially expressed in the retina (C. Z., unpublished data). Overlapping clones were isolated, and a full-length cDNA was constructed. Genomic clones were obtained and used to establish the genomic structure and chromosomal location of *ipp* (Dolph et al., 1993).

Expression and Purification of IPP

A full-length cDNA was cloned into pET3a vector and expressed in BL21 (DE3) cells as described (Studier and Moffatt, 1986). Crude extracts were prepared from the bacterial lysates in 20 mM Tris HCl buffer (pH 7.4). After removal of membranous and particulate material, the extract was loaded on a Mono Q anion FPLC column and eluted with a gradient of 0–1 M NaCl in the same buffer. Active fractions (see below) were pooled, concentrated, and loaded on a Superdex 75 gel-filtration column in the same buffer with 0.5 M NaCl. Pure fractions were pooled, concentrated, and stored at −20°C in 50% glycerol. The enzyme lost little activity over a year.

Activity Measurements of IPP

Inositol polyphosphate 1-phosphatase activity was measured as described by Inhorn and Majerus (1988). The assays were usually initiated by adding the enzyme to a solution containing 50 mM HEPES (pH 7.4), 3 mM $MgCl_2$, 100 mM KCl, 0.5 mM EGTA, and [^{3}H] Ins(1,4)P_2. After incubation, the reaction was loaded onto a Dowex-formate (AG 1-X8) column, and [^{3}H] Ins(4)P eluted with 0.05 M ammonium formate containing 0.1 M formic acid.

Inositol Phosphate Metabolism

Young adult flies were anesthetized with CO_2, beheaded, and immediately homogenized in 50 μl of 50 mM HEPES (pH 7.5), 100 mM KCl, 2 mM $MgCl_2$, 0.5 mM EGTA, 0.1 mM PMSF, 1 μg/ml leupeptin, 1 μg/ml pepstatin, and 1 μg/ml aprotinin. The particulate matter was removed by centrifugation at 14,000 rpm at 4°C for 20 min, and the clear supernatant was incubated with radiolabeled inositol phosphate substrates.

The metabolism of Ins(1,4,5)P_3 and Ins(1,3,4)P_3 was typically estimated by incubating the above extracts with tritiated inositol trisphosphates for 5–30 min. The reactions were terminated by adding 1 ml of ice-cold water and passing the mixture over a 1 ml Dowex-formate AG1-X8 column. The inositol, $InsP_1$, $InsP_2$, and $InsP_3$ fractions were sequentially eluted with water and ammonium-formate/formic acid mixture as previously described (Berridge et al., 1983; Shayman et al., 1987). In all cases, we included a variety of controls, including incubations with heat-inactivated extracts. The eluates were mixed with 10 vol of scintillation liquid (Bio-Safe II) and measured in a scintillation counter.

Antibodies and Microscopy

Antibodies were generated against bacterially expressed protein. The protein was injected into rabbits and the antiserum was affinity purified as previously described (Cassill et al., 1991). The antibody was checked for specificity and affinity using wild-type, mutant, and transgenic controls.

Synaptic boutons were examined by electron micrographic (EM) sectioning as described by Poodry and Edgar (1979). Immnunofluorescence stainings with anti-HRP were carried out as described by Jia et al. (1993). Muscles 6–7 and 12–13 of third instar larvae and tibial NMJs of adult flies were studied for each genotype. In all cases, we analyzed at least five animals per genotype.

Mutant Screen and Western Blots

Males of Canton S genotype were aged for 2 days, chemically mutagenized with ethylmethanesulfonate, and crossed en masse to females containing Df(3R)red^{31}/TM6B. Single F1 males were collected and crossed in single vials to Df(3R)red^{31}/TM6B virgin females. The progeny from this cross bearing mutagenized chromosomes over the deficiency were subjected to a protein immunoblot screen for the loss of the IPP antigen (Dolph et al., 1993, 1994). In essence, single fly heads were excised and sonicated for 3 s in SDS-PAGE buffer. Samples were loaded on 10% SDS-gel electrophoresis (1 head/lane); proteins were allowed to enter the gel for 15 min. Protein from a second line was loaded, and the gel was run for a further 15 min. Protein from a third line was loaded and the run completed. In this way, 45 flies representing 45 individual treated chromosomes could be screened in one gel. The separated proteins were then transferred to a nitrocellulose membrane and incubated with anti-IPP antibody. All experiments involving the mutant flies, including physiological recordings, were also carried out with mutant chromosomes over the deficiency Df(3R)red^{31}. This eliminates any concerns over additional mutations in the *ipp* backgrounds. Wild-type control flies were Canton S.

PCR Reactions

Each of the *ipp* genomic regions from wild-type (Canton S) and mutant flies (*ipp*^{1}, *ipp*^{2}, and *ipp*^{3}) were amplified in multiple independent PCRs to eliminate possible sequence errors occurring during PCR amplification. Sequencing was performed as previously described (Dolph et al., 1993).

DNA Constructs and Transgenic Flies

A 1400 bp *ipp* cDNA fragment containing the entire IPP coding region was cloned into a *Drosophila* transformation vector under the control of the heat-shock promoter (Baker et al., 1994) and injected into wild-type embryos. P element–mediated germline transformations and all subsequent fly manipulations were performed using standard techniques (Karess and Rubin, 1984).

Estimation of Inositol Bisphosphates from Flies

Young adult flies (3 days posteclosion) were fasted for 5 hr and then fed 15 μCi of tritiated inositol in 1% agarose containing 1% sucrose. After 6–12 hr of feeding, flies were transferred to fresh tubes, frozen in liquid N_2, washed in 3 ml of 0.4 M perchloric acid containing 0.5 mM EDTA, and homogenized in 500 μl of the same solution. Samples were centrifuged at 14,000 rpm for 10 min, and the clear supernatant was neutralized to pH 7.4 with 1 M potassium bicarbonate. The extracts were then applied to a Dowex-formate column equilibrated

with water. Inositol, inositol monophosphates, and inositol bisphosphates were eluted sequentially with water, 0.2 M ammonium formate and 0.1 M formic acid, 0.425 M ammonium formate, and 0.1 M formic acid (Berridge et al., 1983; Shayman et al., 1987).

Voltage-Clamp Recording of Postsynaptic Currents

Recordings of excitatory postsynaptic currents in segment A2 or A3 of ventral longitudinal muscle 6 (Crossley, 1978; Campos-Ortega and Hartenstein, 1985) using a two-electrode voltage clamp (OC-725, Warmer Instruments, Hamden, CT) were performed exactly as previously described (Jan and Jan, 1976; Delgado et al., 1992, 1994). In all cases, currents were recorded at a −80 mV holding potential. Current amplitudes and integrals were analyzed using pClamp software. Nerves were cut close to the ventral ganglia and sucked into the stimulating pipette. Evoked currents were elicited by direct stimulation of the nerve at the indicated frequencies by means of a programmable stimulator (Master-8, A.M.P.I., Jerusalem, Israel). Data acquisition and analysis were performed using pClamp software (Axon Istruments, Foster City, CA). Except when indicated, the solution bathing the muscle was made of 128 mM NaCl, 2 mM KCl, 4 mM $MgCl_2$, 0.2 mM $CaCl_2$, 5 mM HEPES, and 36 mM sucrose (pH 7.0). For studies involving lithium, the bath solution contained 118 mM NaCl, 10 mM LiCl, 2 mM KCl, 4 mM $MgCl_2$, 0.2 mM $CaCl_2$, 36 mM sucrose, and 5 mM HEPES (pH 7.0). The stimulation pipette contained 128 mM NaCl, 2 mM KCl, 4 mM $MgCl_2$, 0.2 mM $CaCl_2$, 5 mM HEPES, and 36 mM sucrose (pH 7.0).

Experiments involving analysis of spontaneous end-plate currents were carried out as described in Delgado et al. (1992), except that low temperature recordings were performed at 10°C such that the frequency of spontaneous release is <0.5 events/s. All other experiments were conducted at 25°C.

Release of Neurotransmitter Induced by Hyperosmotic Solution

Following muscle impalement, synaptic connections were visualized with Hoffman optics. A pipette (10 μm tip diameter) filled with an hyperosmotic solution made of 500 mM sucrose, 128 mM NaCl, 2 mM KCl, 4 mM $MgCl_2$, 0.05 mM $CaCl_2$, and 5 mM HEPES (pH 7.0) was placed 20–30 μm above the muscle (Stevens and Tsujimoto, 1995; Rosenmund and Stevens, 1996). Hyperosmotic solution was then released using a picospitzer at 5 psi for 6 or 20 s. During the experiments, the recording chamber (volume = 0.4 ml) was perfused continuously at 0.2 ml/s with normal saline.

Acknowledgments

We thank Ann Becker and Helen Rachmeiler for excellent technical assistance in isolating the *ipp* mutant alleles. We thank Robert Hardy for assistance and advice throughout the course of this investigation. We thank Usha Acharya, Yuki Goda, Chuck Stevens, and members of the Zuker lab for critical reading of the manuscript and helpful advise. This work was supported in part by a grant from the National Eye Institute to C. S. Z. and Fondecyt and a Presidential Chair in Science to P. L. C. S. Z. is an Investigator of the Howard Hughes Medical Institute, and P. L. is an International Scholar of the Howard Hughes Medical Institute.

Received February 24, 1998; revised May 11, 1998.

References

Attree, O., Olivos, I.M., Okabe, I., Bailey, L.C., Nelson, D.L., Lewis, R.A., McInnes, R.R., and Nussbaum, R.L. (1992). The Lowe's oculocerebrorenal syndrome gene encodes a protein highly homologous to inositol polyphosphate-5-phosphatase. Nature *358*, 239–242.

Baker, E.K., Colley, N.J., and Zuker, C.S. (1994). The cyclophilin homolog NinaA functions as a chaperone, forming a stable complex in vivo with its protein target rhodopsin. EMBO J. *13*, 4886–4895.

Bansal, V.S., Inhorn, R.C., and Majerus, P.W. (1987). The metabolism of inositol 1,3,4-trisphosphate to inositol 1,3-bisphosphate. J. Biol. Chem. *262*, 9444–9447.

Baumgartner, S., Littleton, J.T., Broadie, K., Bhat, M.A., Harbecke, R., Lengyel, J.A., Chiquet-Ehrismann, R., Prokop, A., and Bellen, H.J. (1996). A *Drosophila* neurexin is required for septate junction and blood–nerve barrier formation and function. Cell *87*, 1059–1068.

Berridge, M.J. (1993). Cell signalling. A tale of two messengers. Nature *365*, 388–389.

Berridge, M.J., and Irvine, R.F. (1989). Inositol phosphates and cell signalling. Nature *341*, 197–205.

Berridge, M.J., Dawson, R.M., Downes, C.P., Heslop, J.P., and Irvine, R.F. (1983). Changes in the levels of inositol phosphates after agonist-dependent hydrolysis of membrane phosphoinositides. Biochem. J. *212*, 473–482.

Berridge, M.J., Downes, C.P., and Hanley, M.R. (1989). Neural and developmental actions of lithium: a unifying hypothesis. Cell *59*, 411–419.

Broadie, K., Prokop, A., Bellen, H.J., O'Kane, C.J., Schulze, K.L., and Sweeney, S.T. (1995). Syntaxin and synaptobrevin function downstream of vesicle docking in *Drosophila*. Neuron *15*, 663–673.

Broadie, K., Rushton, E., Skoulakis, E.M., and Davis, R.L. (1997). Leonardo, a *Drosophila* 14–3–3 protein involved in learning, regulates presynaptic function. Neuron *19*, 391–402.

Budnik, V., Zhong, Y., and Wu, C.F. (1990). Morphological plasticity of motor axons in *Drosophila* mutants with altered excitability. J. Neurosci. *10*, 3754–3768.

Budnik, V., Koh, Y.-H., Guan, B., Hartmann, B., Hough, C., Woods, D., and Gorczyca, M. (1996). Regulation of synapse structure and function by the *Drosophila* tumor suppresser gene *dlg*. Neuron *17*, 627–640.

Campos-Ortega, J.A., and Hartenstein, V. (1985). The Embryonic Development of *Drosophila melanogaster* (New York: Springer).

Cassill, J.A., Whitney, M., Joazeiro, C.A., Becker, A., and Zuker, C.S. (1991). Isolation of *Drosophila* genes encoding G protein–coupled receptor kinases. Proc. Natl. Acad. Sci. USA *88*, 11067–11070.

Chow, S.C., Ng, J., Nordstedt, C., Fredholm, B.B., and Jondal, M. (1988). Phosphoinositide breakdown and evidence for protein kinase C involvement during human NK killing. Cell Immunol. *114*, 96–103.

Crossley, C.A. (1978). The Morphology and Development of the *Drosophila* Muscular System, Volume 2b, M. Ashburner and T.R.F. Wright, eds. (New York: Academic Press), pp. 449–559.

De Camilli, P., Emr, S.D., McPherson, P.S., and Novick, P. (1996). Phosphoinositides as regulators of membrane traffic. Science *271*, 1533–1539.

Delgado, R., Latorre, R., and Labarca, P. (1992). K^+-channel blockers restore synaptic plasticity in the neuromuscular junction of dunce, a *Drosophila* learning and memory mutant. Proc. R. Soc. Lond. B Biol. Sci. *250*, 181–185.

Delgado, R., Latorre, R., and Labarca, P. (1994). Shaker mutants lack posttetanic potentiation at motor end-plates. Eur. J. Neurosci. *6*, 1160–1166.

Dolph, P.J., Ranganathan, R., Colley, N.J., Hardy, R.W., Socolich, M., and Zuker, C.S. (1993). Arrestin function in inactivation of G protein–coupled receptor rhodopsin in vivo. Science *260*, 1910–1916.

Dolph, P.J., Man Son Hing, H., Yarfitz, S., Colley, N.J., Deer, J.R., Spencer, M., Hurley, J.B., and Zuker, C.S. (1994). An eye-specific G beta subunit essential for termination of the phototransduction cascade. Nature *370*, 59–61.

Fukuda, M., and Mikoshiba, K. (1997). The function of inositol high polyphosphate binding proteins. Bioessays *19*, 593–603.

Gee, N.S., Reid, G.G., Jackson, R.G., Barnaby, R.J., and Ragan, C.I. (1988). Purification and properties of inositol-1,4-bisphosphatase from bovine brain. Biochem. J. *253*, 777–782.

Geffner, J.R., Giordano, M., Serebrinsky, G., and Isturiz, M.A. (1988). Different activation pathways involved in antibody-dependent and immune-complexes–triggered cytotoxicity mediated by neutrophils. Clin. Exp. Immunol. *74*, 471–476.

Inhorn, R.C., and Majerus, P.W. (1988). Properties of inositol polyphosphate 1-phosphatase. J. Biol. Chem. *263*, 14559–14565.

Jan, L.Y., and Jan, Y.N. (1976). Properties of the larval neuromuscular junction in *Drosophila melanogaster*. J. Physiol. (Lond.). *262*, 189–214.

Jia, X., Gorczyca, M., and Budnik, V. (1993). Ultrastructure of neuromuscular junctions in *Drosophila*: comparison of wild type and mutants with increased excitability. J. Neurobiol. *24*, 1025–1044.

Karess, R.E., and Rubin, G.M. (1984). Analysis of P transposable element functions in *Drosophila*. Cell *38*, 135–146.

Lin, T., Orrison, B.M., Leahey, A.M., Suchy, S.F., Bernard, D.J., Lewis, R.A., and Nussbaum, R.L. (1997). Spectrum of mutations in the OCRL1 gene in the Lowe oculocerebrorenal syndrome. Am. J. Hum. Genet. *60*, 1384–1388.

Majerus, P.W. (1992). Inositol phosphate biochemistry. Annu. Rev. Biochem. *61*, 225–250.

Majerus, P.W. (1996). Inositols do it all. Genes Dev. *10*, 1051–1053.

McPherson, P.S., Garcia, E.P., Slepnev, V.I., David, C., Zhang, X., Grabs, D., Sossin, W.S., Bauerfeind, R., Nemoto, Y., and De Camilli, P. (1996). A presynaptic inositol 5-phosphatase. Nature *379*, 353–357.

Nishizuka, Y. (1992). Intracellular signaling by hydrolysis of phospholipids and activation of protein kinase C. Science *258*, 607–614.

Nussbaum, R.L., Orrison, B.M., Janne, P.A., Charnas, L., and Chinault, A.C. (1997). Physical mapping and genomic structure of the Lowe syndrome gene OCRL1. Hum. Genet. *99*, 145–150.

Okabe, I., and Nussbaum, R.L. (1995). Identification and chromosomal mapping of the mouse inositol polyphosphate 1-phosphatase gene. Genomics *30*, 358–360.

Parissenti, A.M., Kirwan, A.F., Kim, S.A., Colantonio, C.M., and Schimmer, B.P. (1996). Molecular strategies for the dominant inhibition of protein kinase C. Endocr. Res. *22*, 621–630.

Petersen, S.A., Fetter, R.D., Noordermeer, J.N., Goodman, C.S., and DiAntonio, A. (1997). Genetic analysis of glutamate receptors in *Drosophila* reveals a retrograde signal regulating presynaptic transmitter release. Neuron *19*, 1237–1248.

Poodry, C.A., and Edgar, L. (1979). Reversible alterations in the neuromuscular junctions of *Drosophila melanogaster* bearing a temperature-sensitive mutation, *shibire*. J. Cell Biol. *81*, 520–527.

Ranganathan, R., Malicki, D.M., and Zuker, C.S. (1995). Signal transduction in *Drosophila* photoreceptors. Annu. Rev. Neurosci. *18*, 283–317.

Rosenmund, C., and Stevens, C.F. (1996). Definition of the readily releasable pool of vesicles at hippocampal slices. Neuron *16*, 1197–1207.

Shayman, J.A., Morrison, A.R., and Lowry, O.H. (1987). Enzymatic fluorometric assay for myo-inositol trisphosphate. Anal. Biochem. *162*, 562–568.

Shears, S.B. (1992). Metabolism of inositol phosphates. Adv. Second Messenger Phosphoprotein Res. *26*, 63–92.

Shears, S.B. (1996). Inositol pentakis- and hexakisphosphate metabolism adds versatility to the actions of inositol polyphosphates. Novel effects on ion channels and protein traffic. Subcell. Biochem. *26*, 187–226.

Stevens, C.F., and Tsujimoto, T. (1995). Estimates for the pool size of releasable quanta at a single central synapse and for the time required to refill the pool. Proc. Natl. Acad. Sci. USA *92*, 846–849.

Streb, H., Irvine, R.F., Berridge, M.J., and Schulz, I. (1983). Release of Ca^{2+} from a nonmitochondrial intracellular store in pancreatic acinar cells by inositol-1,4,5-trisphosphate. Nature *306*, 67–69.

Studier, F.W., and Moffatt, B.A. (1986). Use of bacteriophage T7 RNA polymerase to direct selective high-level expression of cloned genes. J. Mol. Biol. *189*, 113–130.

Thomas, U., Kim, E., Kuhlendahl, S., Koh, Y.H., Gundelfinger, E.D., Sheng, M., Garner, C.C., and Budnik, V. (1997). Synaptic clustering of the cell adhesion molecule Fasciclin II by Discs-Large and its role in the regulation of presynaptic structure. Neuron *19*, 787–799.

Timar, J., Raso, E., Fazakas, Z.S., Silletti, S., Raz, A., and Honn, K.V. (1996). Multiple use of a signal transduction pathway in tumor cell invasion. Anticancer Res. *16*, 3299–3306.

York, J.D., and Majerus, P.W. (1990). Isolation and heterologous expression of a cDNA encoding bovine inositol polyphosphate 1-phosphatase. Proc. Natl. Acad. Sci. USA *87*, 9548–9552.

York, J.D., Veile, R.A., Donis, K.H., and Majerus, P.W. (1993). Cloning, heterologous expression, and chromosomal localization of human inositol polyphosphate 1-phosphatase. Proc. Natl. Acad. Sci. USA *90*, 5833–58377.

York, J.D., Chen, Z.W., Ponder, J.W., Chauhan, A.K., Mathews, F.S., and Majerus, P.W. (1994). Crystallization and initial X-ray crystallographic characterization of recombinant bovine inositol polyphosphate 1-phosphatase produced in *Spodoptera frugiperda* cells. J. Mol. Biol. *236*, 584–589.

Zhang, X., Jefferson, A.B., Auethavekiat, V., and Majerus, P.W. (1995). The protein deficient in Lowe syndrome is a phosphatidylinositol-4,5-bisphosphate 5-phosphatase. Proc. Natl. Acad. Sci. USA *92*, 4853–4856.

Zhong, Y., and Wu, C.-F. (1990). Altered synaptic plasticity in *Drosophila* memory mutants with a defective cyclic AMP cascade. Science *251*, 198–201.

GenBank Accession Number

The GenBank accession number for the Drosophial ipp gene is AF069513.